

CALIBRATION OF COHESIVE DEM PARAMETERS UNDER RAPID FLOW CONDITIONS AND LOW CONSOLIDATION STRESSES

Mohsin Ajmal¹, Thomas Rößler¹, Micheal Carr² and Andre Katterfeld¹

¹ University of Magdeburg,
Chair of Material Handling
Universitätsplatz 2, 39104 Magdeburg, Germany
mohsin.ajmal@ovgu.de

² Centre for Bulk Solids and Particulate Solids
(CBSPT), Newcastle/AU

Keywords Granular Materials, Cohesion, DEM, Calibration, JKR,

Abstract Discrete Element Method (DEM) is a well-established and validated tool for the simulation of bulk materials. However, a lot of questions still need answering in the domain of cohesion and adhesion. Cohesive materials display a wide range of distinct and elusive properties which contribute towards their reduced flowability.

The JKR model is one of the most widely used models in this realm which takes into account Surface Energy Density and increased particle overlap to explain cohesion. The ambiguity associated with Surface Energy or Interfacial Energy is tackled by developing thorough calibration procedures which will help in fine tuning these parameters. One of the limitations of DEM is the usage of reduced Young's Modulus to capture collision time scales for a stable simulation in manageable computational times. Reducing the Young's Modulus in a cohesive JKR simulation usually leads to unrealistic overlaps which can be mitigated by also reducing the Surface Energy Density.

In recent years systematic parameter calibration and validation endeavours have quite successfully tried to answer those questions on a macroscopic level. This work focuses on an analytically driven calibration protocol using draw down and angle of repose tests which can be classified as uniaxial low consolidation tests. Hence, complications due to high compaction stresses can be neglected. Cohesive DEM parameters will be calibrated using a combination set of Friction coefficients, Young's Modulus and Surface Energy Density. The calibration protocol also aids in deciding to which extent these parameters can be reduced in order to get good agreement between simulation and experiment. Further investigations will be carried out to assess the effect of cohesion and adhesion on rolling resistance. The JKR model is used during the exercise due to its robustness, manageable computational times and a relatively wide area of application. This will allow to narrow down on a unique set of parameters for different materials.

1 INTRODUCTION

In order to design efficient bulk solid handling equipment, Discrete Element Method (DEM) is employed as a very robust and widely used tool for simulating material flows[1]. Simulation of fine granular materials is extremely time consuming with currently available computational resources, as the particle sizes are in the range of microns. DEM models for industrial applications are typically idealized in terms of the considered particle size, shape and stiffness. Due to this idealisation, calibration in DEM is required and has become a frequently used approach.

Calibration exercises try to bridge the gap between idealization and reality by comparing experimental results with simulations, which are conducted over a carefully chosen parameter field. A matching response between simulations and experiments can be found in this way, allowing to implement the narrowed down ambiguous parameter set in real world applications with satisfactory results.

Valuable work in the field of calibration and validation has been undertaken by [3], [4], [5],[6]. One of the major draw backs of this approach is that it involves a lot of trial and error, henceforth a large number of simulations are required. HPCs are therefore a valuable tool to run several simulations in parallel. This allows for a thorough analysis of the parameter fields. Implementation of optimization and A.I algorithms ([7],[8],[9],[10]) can further reduce the time required for computations.

During calibration exercises further complications may arise when calibrating cohesive materials as some experiments used for cohesion less bulk material characterization might not give satisfactory results with cohesive materials. Additional parameters such as Surface energy density must also be analysed in parallel, which further increases the number of simulations required to obtain acceptable calibration results. Cohesive materials are especially difficult to handle, therefore significant problems occur in industry due to blockages in equipment such as hoppers, chutes, feeders and conveyors.

This paper focuses on developing a calibration protocol for cohesive bulk materials such as wet sand using a draw down experiment. It was observed that at smaller opening sizes the material was unable to flow and resulted in material-arching at the opening. By defining different openings of the draw down experimental set-up, limits for blockage and free flow of bulk materials can be specified in both simulation and experiments. Wet sand with a Moisture Content (MC) of 10% is used for the experimental measurements.

2 METHODS AND MODELS

2.1 Contact Models

As in most DEM simulations, the Hertz-Mindlin contact model is used and rolling friction is according to [2]. The choice of time step is critical as it can have a profound effect on the simulation behavior. 15% of Rayleigh time was used as the simulation time step, as it is a widely well-established criterion for DEM simulations.

Table 1: Parameter and Model Selection for DEM Simulations

Parameter	Value	Description
Contact models		Hertz-Mindlin SJKR Modified elastic plastic spring dashpot model , Wensrich et. al[2]
Particle density (kg/m ³)	2083	Experiment
Young's Modulus (Pa)	1E8	Aproximation; reduction
Poisson's ratio	0.3	Approximation
Coefficient of restitution	0.2	Approximation
Particle-wall friction coefficient	0.41	Experiment
Time step (s)		15% of Rayleigh time
Gravity (m/s ²)	9.81	Global value

2.2 The Johnson-Kendell-Roberts (JKR) Model

Johnson et al. [11] tries to explain cohesion using the surface energy density while others use liquid bridging or water content of individual particles to explain the sticky materials[12]. Easo and Wassgren [13] used a combination of different models for liquid bridging and surface tension. Two major phenomenon which contribute to cohesion are material bridging and inter-molecular interaction. Particles in the range of micro meters to nanometers are more influenced by Wan-der-waals forces or electrostatic forces. Therefore, it becomes quite important to identify the governing cohesion mechanism at the start of each calibration exercise.

Table 2: Cohesion Mechanism ([14])

Without material bridges	With material bridges	
	Liquid bridges	Solid Bridges
<ul style="list-style-type: none"> • Electrostatic interaction 	<ul style="list-style-type: none"> • Free moveable liquid surface <ul style="list-style-type: none"> ○ Capillary Forces ○ Interfacial Forces 	<ul style="list-style-type: none"> • Sintering
<ul style="list-style-type: none"> • Van-der-Waals Forces • Valence bond 	<ul style="list-style-type: none"> • Not moveable binder bridges <ul style="list-style-type: none"> ○ Binder ○ Glue ○ Absorption Forces 	<ul style="list-style-type: none"> • Grain Growth • Crystallization

Johnson-Kendell and Roberts [11] developed a model in 1971 which further extends the Hertz model to take into account the effect of tensile forces at the contact area edges to explain the cohesive behavior. According to this model the total force, F_{all} , acting at the contact point

of the two particles is given by:

$$F_{\text{all}} = F_{\text{ext}} + 3\gamma\pi R + \sqrt{3\gamma\pi R F_{\text{ext}} + (3\gamma\pi R)^2} \quad (1)$$

Where, F_{ext} is the external normal force acting on the particle, γ is the cumulative surface energy density, and R is the effective radius for the particle radii R_1 and R_2 . The radius of contact a as proposed by JKR theory becomes:

$$a^3 = \frac{R}{K} (F_{\text{ext}} + 3\gamma\pi R + \sqrt{6\gamma\pi R F_{\text{ext}} + (3\gamma\pi R)^2}) \quad (2)$$

The cumulative surface energy is given by:

$$\gamma = \gamma_1 + \gamma_2 - 2\gamma_{12} \quad (3)$$

here, γ_1 and γ_2 are the intrinsic surface energies (J/m^2) of the two particles and γ_{12} is the interfacial energy. With an attractive surface energy, a force is required to separate the spheres. This force is generally referred to as work of adhesion [11],

$$F_c = 3\pi\gamma R \quad (4)$$

This work of cohesion or pull force, F_c , is independent of the elastic contact properties of the particles. When taking into account the surface energy at contact this model predicts that the force at the contact is changed from Hertzian contact to a more cohesive contact. Chokshi et al. [15] proposed a modified equation for the JKR model which is the bases of the simplified JKR model implemented in LIGGGHTS®.

$$F = \frac{4Ea^3}{3R} - 2\pi a^2 \sqrt{\frac{4\gamma E}{\pi a}} \quad (5)$$

This simplified approach reduces the computational time by combining together surface energy, young's modulus and contact radius into one parameter 'Cohesion Energy Density (CED)'. Investigations prior to this work have shown that with high CED values and low Young's modulus the particles implode into each other leading to highly unstable systems. This may be due to the fact that a reduction in stiffness of the particles is unable to counteract the effects of high attractive forces leading to unrealistic overlaps. A relation given by [16] explains the reduction of surface energy with respect to young's modulus which is given by:

$$\gamma_{\text{mod}} = \gamma \left(\frac{E_{\text{mod}}}{E} \right)^{2/5} \quad (6)$$

3 EXPERIMENTAL SETUP

A draw-down experimental set-up, as proposed by [17], [18], [19], was used for the calibration of wet sand. It consists of two boxes made of Perspex, their dimensions are shown in Figure 1. The depth of the top box is 100mm and the lower box is 180mm. Flaps are installed at the bottom opening of the top box, which can be opened instantaneously, so that the material flows un-obstructed from the top box and the errors related to delayed opening can be reduced. To measure the flow rate of the material from the top box, it is placed on load cells. As the material flows out from the top box a shear angle is formed in the top box, while a heap is

formed at the bottom which is a good indication of the angle of repose. The material under investigation was filled up to a height of 300mm in the top box. The shear angle (degree), φ_{DD} , in the top box and the angle of repose (degree), β_{DD} , in the bottom box were measured through image analysis. Each experiment was repeated three times. In Table 3, the results of the experiments are presented.

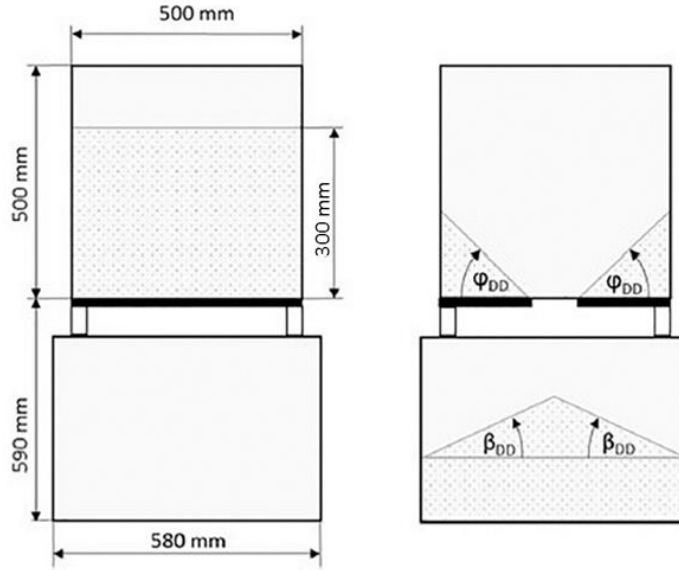


Figure 1: Schematic of draw down apparatus.

Table 3: Experimental Results

	Angle of Repose β_{DD} (AOR) [degree]	Mass loss [kg]
Opening 90 mm	1.75	0.47
Opening 120 mm	28.7	7.23
Opening 150 mm	30.1	7.79

4 DEM PARAMETER CALIBRATION

4.1 Simulation Set-up

The open-source DEM programme LIGGGHTS[®] was used during the calibration exercise. It is computationally not possible to simulate wet-sand with real particle size distributions as they are in the ranges of micro-meter to nano-meter. A scaling factor of 10 was used during the simulation. The scaled-up particles were about 10 times smaller than the opening size. This ensures that blocking due to scale-up will not occur.

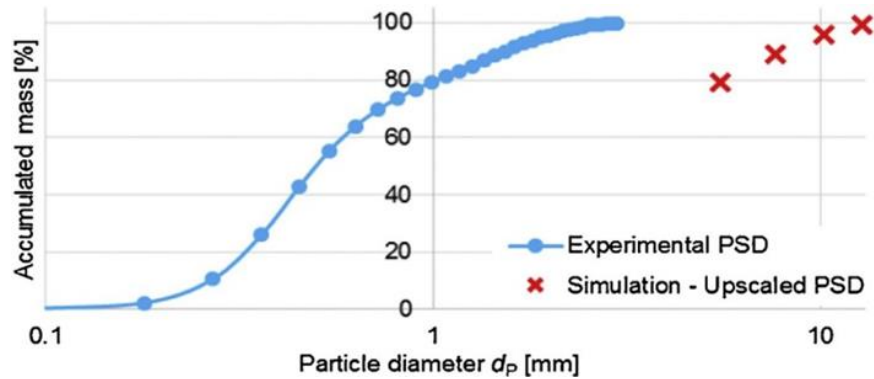


Figure 2: Particle size distribution comparison.

A parameter set of μ_{p-p} (particle-to-particle friction), μ_r (co-efficient of rolling friction), CED (Cohesion Energy Density) was analysed. For simplification AED (Adhesion Energy Density) value was kept the same as CED value. Mass loss in the top box and the angle of repose in the bottom box were measured, by systematically varying the parameter field in order to narrow down on a set of unique values which shows good agreement with the experimental results.

Every simulation was undertaken with a particle count of approximately 95000 particles. The simulation time was set to a constant 6 seconds. Simulations for opening sizes of 90 mm and 150 mm were performed and later the same simulation approach was applied to opening size 120 mm to get more refined results for the developed approach. These were then compared together to get the best possible agreement. The calibration was undertaken according to the procedure shown in Figure 3.

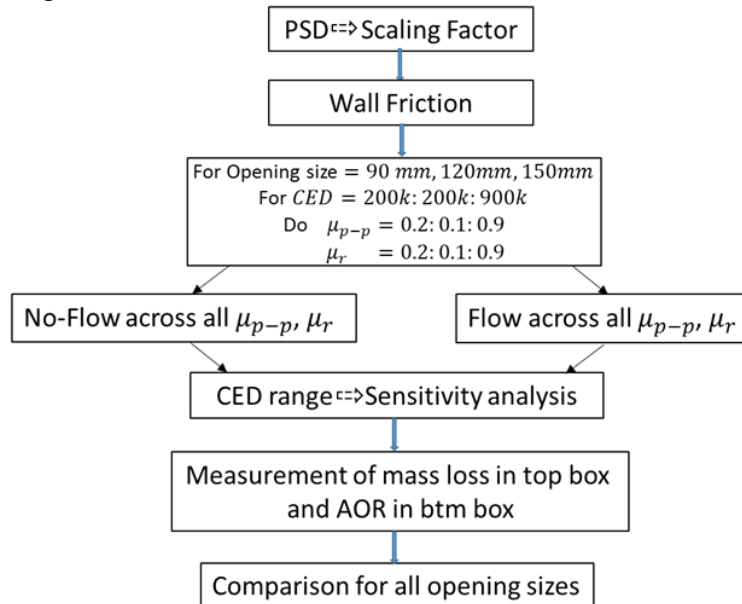


Figure 3: Calibration protocol using the draw down testing apparatus

4.2 Simulation Results

In order to narrow down on a unique set of parameters, which represents the up-scaled particles, a large number of simulations were performed (approx. 1500) in parallel on the OvGU HPC Neumann.

CED values corresponding to no flow and sure flow were taken as the lower and the upper limits respectively. A sensitivity analysis between these limits was then undertaken in order to narrow down on the value of CED, which results in an overlap agreement for all possible parameter combinations. The lower limit corresponds to the phenomenon when there is flow from the opening sizes of 120 mm and 150 mm at all combinations of μ_{p-p} and μ_r . In the experiments mass loss from these opening sizes and arching at opening sizes of 90 mm and below were recorded. This criteria can be different for different materials and should be investigated in the experiments. The upper limit on the other hand shows no flow or arching at even the lowest possible combination of μ_{p-p} and μ_r .

It was further observed that changing AED values also led to differences in the material behavior inside the apparatus. This strengthens our understanding that wall effects also play a major role in the flow or the loss of material from the top box.

Figure 4 shows the results of mass loss in the top box and angle of repose AOR for CED 700000 for the three opening sizes. The AOR in simulations was measured with the same algorithm used in [6]. The limits of the highlighted areas in the contour plots were chosen $\pm 10\%$ of the average experimental values, this percentage is same as the experimental deviation of the results.

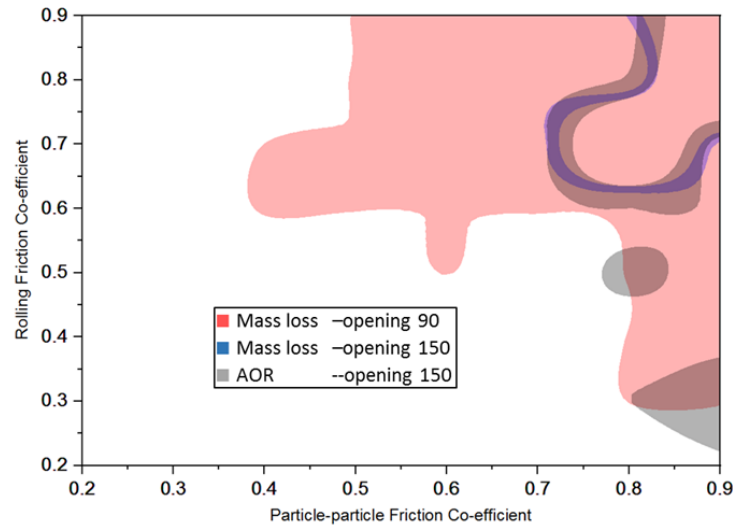


Figure 4: Contour plot for opening 150 mm

The simulations undertaken in the first phase resulted in similar contour areas for mass loss and angle of repose for an opening size of 150 mm. The red area shows the region where arching occurs with an opening size of 90 mm. The overlaying of result for two opening sizes with repeatable arching and outflow behavior shows that based on these two tests it is not possible

to identify a unique parameter set which results in the same mass loss and AOR.

In order to get a more refined area of our parameter set the same simulations were repeated for an opening size of 120 mm (see Figure 5 left). Overlapping these two plots results in a common area which can be identified as the best possible solution for the three opening sizes. In this way it was found possible that a unique set of parameters can be identified which fit most of the scenarios for the SJKR model. Figure 5 right shows a common overlap area (marked by red circle in bottom figure) at approximately $\mu_{p-p} = 0.7$ and $\mu_r = 0.8$, giving the required parameter set for wet sand calibration. Figure 6 shows the direct comparison of experimental and simulation results of the draw down test after the flow of the material has finished.

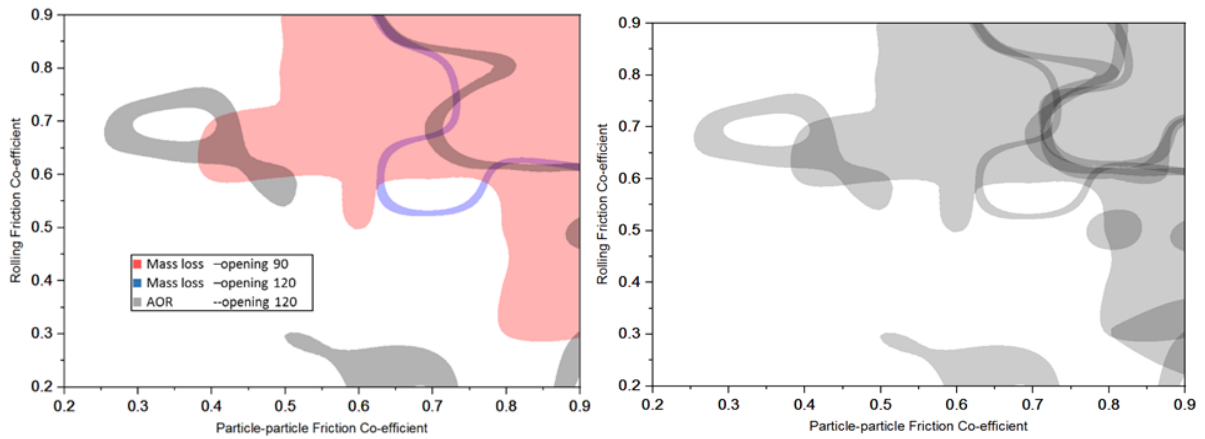


Figure 5: (left) Contour plot for opening 120 mm; (right) Overlap of both plots.

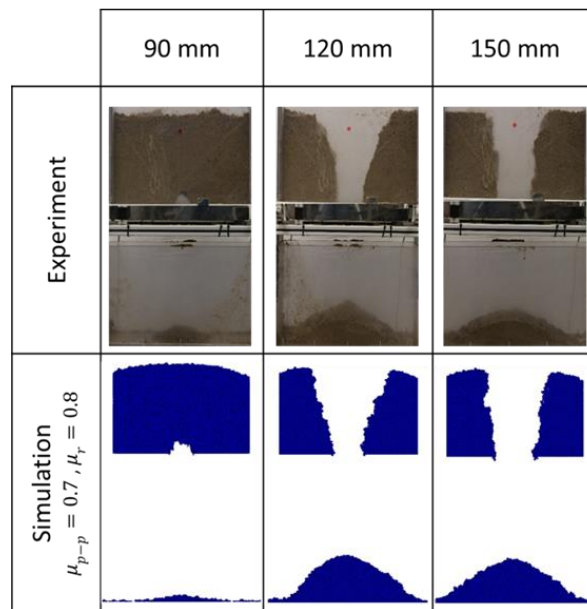


Figure 6: Comparison of experimental and simulation results for the acquired best fitted parameter set (CED=700k J/m³).

Table 4: Comparison of Experimental and Simulation Results

Opening size (mm)	Mass loss (kg)		Shear Angle (degree)		Angle of repose (degree)	
	Experimental	Simulation	Experimental	Simulation	Experimental	Simulation
90	0.47	0.43	N/A	N/A	1.75	1.25
120	7.23	8.36	78.57	77.49	28.7	40.35
150	7.79	8.77	84.51	83.03	30.1	35.1

Table 4 shows the comparison between experimental and simulation results for the obtained parameter set. The experimental and simulation regime was undertaken using a low consolidation approach. High consolidated cohesive materials behave similar to a solid structure, which is very difficult to simulate and quantify. Efforts are made to avoid consolidation of bulk material in practical applications, however it is quite difficult to prevent. A thorough study has been undertaken in this work to analyse all possible parameters which can contribute to an eventual progress towards consolidation of cohesive bulk material in practical application, allowing us to avoid this eventuality.

5 Conclusion

From the obtained results it is clear that a satisfactory agreement for simulations and experiments was achieved. However, it also became clear, that more tests (at least 3) are necessary to achieve a single parameter set. Draw down experimental measurements can therefore be used not only for free flowing bulk materials but also to calibrate cohesive materials using the SJKR model. The following examinations would be beneficial in terms of improving and further validating the presented method.

- Other cohesive contact models such as the Edinburgh Elasto-Plastic Adhesion ‘EEPA’ contact model and ‘Easo’ liquid bridging contact models are available in LIGGGHTS® which can also be studied in this context, especially in the area of particle-wall adhesion
- Implementation and study of the JKR model in its entirety, albeit for the narrowed down parameter set.
- Study of further cohesive rolling resistance models.
- Study the effect of AED in detail.

REFERENCES

- [1] Chen, W., Roberts, A., Williams, K., Miller, J., & Plinke, J. (2017). On uniaxial compression and Jenike direct shear testings of cohesive iron ore materials. *Powder Technology*, 312, 184–193.
- [2] Wensrich, C., Katterfeld, A. (2012) Rolling Friction as a Technique for Modelling Particle Shape in DEM. In: *Powder technology*. Volume 217, Pages 409–417
- [3] Gröger, T., Katterfeld, A. (2006). On the Numerical Calibration of Discrete Element

Models for the Simulation of Bulk Solids. *Computer Aided Chemical Engineering* 21

[4] Grima, A. P., Wypych, P. W. (2011). Development and validation of calibration methods for discrete element modelling. *Granular Matter*, 13(2), 127–132.

[5] Coetzee, C. J. (2016). Calibration of the discrete element method and the effect of particle shape. *Powder Technology*, 97, 50–70.

[6] Roessler, T., Richter, C., Katterfeld, A., (2019). Will, F.: Development of a standard calibration procedure for the DEM parameters of cohesionless bulk materials—part I: Solving the problem of ambiguous parameter combinations, *Powder Technology* 343 803–812

[7] Rackl, M., Hanley, K. J., (2017) . A methodical calibration procedure for discrete element models. *Powder Technology* 307 73–83.

[8] Do, H.Q., Aragón, A.M., Schott, D.L., (2018). A calibration framework for discrete element model parameters using genetic algorithms, *Adv. Powder Technol.* 29 1393–1403 Nr. 6, S.

[9] Roessler, T., Richter C., Katterfeld, A. (2018). Will, F.: Standardverfahren zur multikriteriellen Kalibrierung von DEM-Parametern von kohäsionslosen Schüttgütern unter Verwendung eines Optimierungsalgorithmus. In: *Fachtagung Schüttgutfördertechnik 2018*. Technische Universität München, S. 53-76

[10] Benvenuti, L., Kloss, C., & Pirker, S., (2016) Identification of DEM simulation parameters by Artificial Neural Networks and bulk experiments. *Powder Technology* 291 456–465.

[11] Johnson, K. L., Kendall, K., Roberts, A. D, (1971) Surface energy and the contact of elastic solids. *Proceedings of the Royal Society of London Series A* 324 301–313.

[12] Shi, D., McCarthy, J.J., (2008). Numerical simulation of liquid transfer between particles, *Powder Technology* 184 64–75

[13] Easo, L. A., Wassgren, C. (2013) Comparison of liquid bridge volume models in DEM simulations. Retrieved from:
<https://aiche.confex.com/aiche/2013/webprogram/Paper312290.html>

[14] Rumpf, H. (1958). Grundlagen und methoden des granulierens. *Chemie Ingenieur Technik*, 30(3), 144–158.

[15] Chokshi, A., Teilens, A.G.G.M., Hollenbach, D., (1993). Dust Coagulation, *The Astrophysical Journal* 407 809-819

[16] Hærvig, J., Kleinhans, U., Wieland, C., Spliethoff, H., Jensen A.L., Sørensen, K., Condra, T.J., (2017). On the adhesive JKR contact and rolling models for reduced particle stiffness discrete element simulations, *Powder Technology* 319, 472-482

[17] Roessler, T., Katterfeld, A., (2019). DEM parameter calibration of cohesive bulk materials using a simple angle of repose test, *Particuology* 343 803–812

[18] Chen, W., Roberts, A., Katterfeld, A., Wheeler, C., (2018). Modelling the stability of iron ore bulk cargoes during marine transport, *Powder Technology* 326 255–26

[19] Carr, M., Wheeler, C., Williams, K., Katterfeld, A., Elphick, G., Nettleton, K., Chen, W., (2018). Discrete element modelling of problematic bulk materials onto impact plates. In: *CHoPS 2018: 9th International Conference for Conveying and Handling of Particulate Solids*, Greenwich Maritime Campus, London, 10-14 September 2018 - London, insges. 6 S.